

Automatic ROI Extraction and Vein Pattern Imaging of Dorsal Hand Vein Images

B. M. Sontakke¹, V. T. Humbe², P. L. Yannawar³

¹College of Computer Science & IT, Latur, (MS) India

²School of Technology, S.R.T.M.U, Sub Campus Latur, (MS) India

³Department of Computer Science and IT, Dr. B.A.M.U, Aurangabad (MS) India.

Abstract- *The dorsal hand-vein pattern is one of the human biometric signatures that can be used for personal verification. The first task of a verification process using hand-vein patterns is extracting the pattern from an infrared hand vein image. But before extracting the vein pattern we have to get the Region of interest. In hand vein imaging, region of interest (ROI) refers to the portion of an image that contains the most important and useful information. Therefore next step is to emphasis on extracting ROI for effectively performing following steps of the vein enhancement system. In general, the propose ROI extraction method involves Hand region segmentation, Boundary tracing, Reference point determination, features point selection, Established ROI coordinates and ROI extraction.*

Keywords- Biometrics, Dorsal hand Vein, ROI, Image Enhancement, ROI techniques

I. INTRODUCTION

Biometric recognition systems are very popular now a days because they contain properties like universality, uniqueness, stability and strong immunity to forgery. Meanwhile the hand veins lie below the skin and are, mostly not visible to open eye, they provide a strong resistance against counterfeit. The complex vascular pattern present inside the hand allows the computation of a good set of features that can be used for personal identification. After acquiring the hand vein images, we first need to extract region of interest (ROI) images from the original images. In 2001, Han et al. proposed a method that localized the ROI by using the feature points of the hand which were the pits between two fingers [1]. Li et al. proposed a hand boundary-based ROI localization method [2]. In 2003, Kumar et al. proposed an ellipse fitting-based method to extract the ROI [3]. Han proposed a method to extract ROI by calculating the centroid of the hand in 2007 [4]. However, these methods need very clear and high-quality hand vein images. So they can work well only for high resolution images. For low resolution hand vein images, the existing methods cannot completely well extract the ROI images.

In this paper, a ROI extraction algorithm and vein pattern imaging method are proposed. We use this system and algorithm for hand vein pattern imaging and ROI extraction, and use the obtained ROI images for hand vein recognition. To fix the position of the ROI of vein images firstly needs to build a coordinate system which uses low and right borders of the hand as the x axis and y-axis respectively. The proposed algorithm shows excellent performance in extracting the ROI of the hand vein images with low resolution. We used the acquired images to build a hand vein database. This database and another hand vein database are used to test our ROI extraction algorithm. Our tentative results show that from different hand vein images we extracted the ROI images successfully. We also use the extracted ROI images for hand vein recognition and the experiments demonstrated the effectiveness of the proposed system and algorithm and our method can achieve satisfactory performance on hand vein pattern imaging, ROI extraction.

The rest of this paper is organized as follows. Section II and III introduces the hand vein ROI extraction algorithm in detail. Section IV describes hand vein pattern imaging. Experimental Result is shown in Section V. Section VI offers our conclusion.

II. HAND VEIN ROI EXTRACTION ALGORITHM

- 1) Smooth the original images by using the Gaussian low-pass filter. In the experiments, we use the Gaussian low-pass filter with the size of 3×3 and $\sigma = 1.5$.
- 2) Binarize the smoothed images. In the experiments, the binarization threshold is set to 0.75.
- 3) Detect the edges of the binary images by using the canny operator.
- 4) Thin the edge images.
- 5) To extract the ROI, four coordinates have to be determined. The first coordinate, P1 is established at the middle point between the second finger-web and the first additional feature point. Next, P2 is located at the middle point between fourth finger-web and the second additional point.

- 6) The extraction of ROI begins by cropping to obtain the loose areas as indicated by yellow lines, our algorithm determines the ROI with the size of 60x60 pixels.
- 7) Generate the ROI images in accordance with the size and position of the ROI determined by Step (6).

III. HAND VEIN ROI EXTRACTION

The important and useful information from the part of an image that is called as ROI from hand vein imaging. Therefore emphasis is on extracting ROI for effectively perform following steps of the vein enhancement system.

In general, the propose ROI extraction method involves six steps. The details of each step are described in the following sub-sections.

A. Hand Region Segmentation

The ROI extraction begins with finding the optimal grey- level threshold values, in an image histogram using Otsu's thresholding [5]. The hand region and the background are the two main parts that is segmented by the threshold value. The hand region and the background are the two main parts that is segmented by the threshold value. Once the optimal threshold value is obtained, the two optimal parts can be identified and separated.

B. Boundary Tracing

We have used Boundary tracing algorithm to separate the hand region (i.e. nonzero pixel area) from the background (zero pixel area) to extract hand contour from binary image.

C. Reference Point Determination

After a hand contour is obtained, the next stage is calculation of Euclidean distance to measure the distance between BPV from its reference point. The border pixel vector (BPV) means all visited pixel points on the contour. Before the Euclidean distance can be computed, a reference point must can be selected. The reference point is the intersection line formed by the mid-point of hand wrist and bottom margin of a hand image.

D. Features Point Selection

After calculation of the Euclidean distance between BPV and reference point, distance distribution diagrams are constructed to select feature points. The pattern of distribution diagram is rather similar to the geometric shape of a hand where the local maxima represent the finger-tips and local

minima represent the finger -webs. As a result, a total of five local maxima (indicated by red points in Fig. 1(a)) and four local minima (indicated in green points in Fig. 1(b)), are selected as feature points.

In order to establish a larger size of ROI, two additional points are proposed, indicated in yellow points in Fig. 1(c). The first additional point is determined based on the mirror image distance between the second finger-web and second finger-tip. The second additional point is determined based on the mirror image distance of the fourth finger-web and the fifth finger-tip.

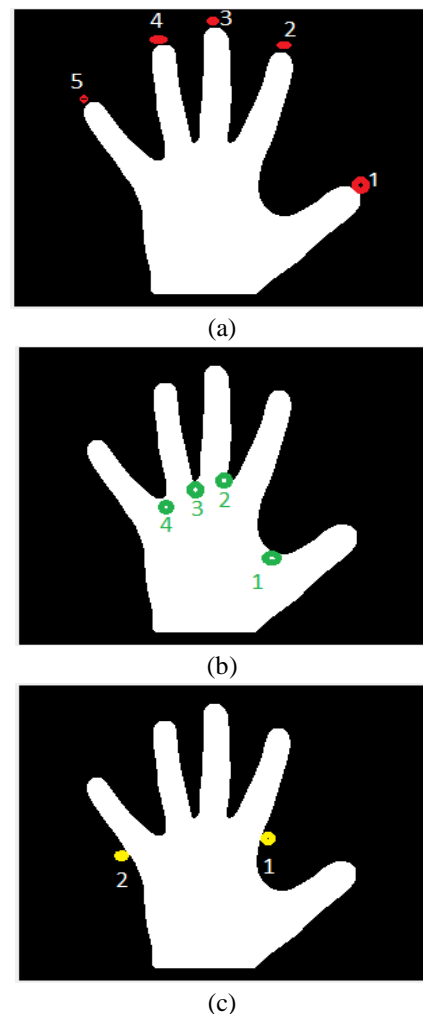
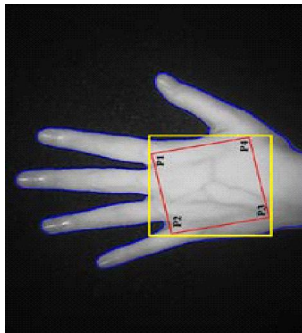


Fig. 1 Features points (a) local maxima (b) local minima and (c) additional points

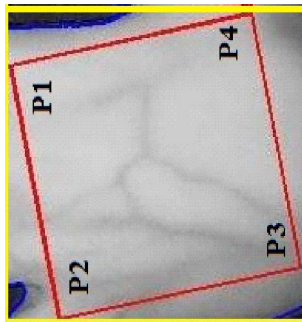
E. Established ROI Coordinates

To extract the ROI, four coordinates have to be determined as illustrated in Fig. 2(a). The first coordinate, P1 is established at the middle point between the second finger-web and the first additional feature point. Next, P2 is located

at the middle point between fourth finger-web and the second additional point. Then, P3 is obtained 90° clockwise using linear transformation from coordinate of P2 with a distance equal to the line constitute by P1–P2. The same procedure is applied in order to obtain P4 based on 90° counter-clockwise from coordinate of P1. As a result, ROI is defined as a square region of P1P2P3P4 as shown in Fig. 2(a).



(a)



(b)

Fig 2 (a) Detected ROI in hand image and (b) cropped ROI with loose area.

F.ROI Extraction

The extraction of ROI begins by cropping to obtain the loose areas as indicated by yellow lines in Fig. 2(a). It contains all ROI coordinates, P1, P2, P3 and P4. Fig. 2(b) shows an example of cropped ROI region for detected ROI in Fig. 2(a). Then the cropped ROI area is rotated at an angle θ to a standard orientation as illustrated by the dotted lines in Fig. 3. To do this, the angle θ is calculated using MATLAB Four-Quadrant Inverse Tangent function, atan2.

Figure 4(a) shows an example of cropped ROI before being rotated. Figure 4(b) shows ROI of P1, P2, P3 and P4 in a standard orientation after θ rotation using MATLAB imrotate. Finally, a square region of ROI is automatically cropped using MATLAB function imcrop to obtain an ROI as shown in Figure 4(c).

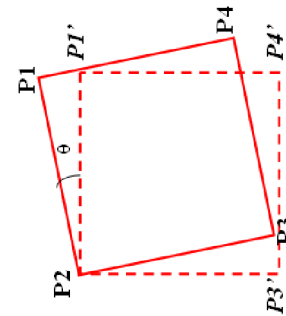
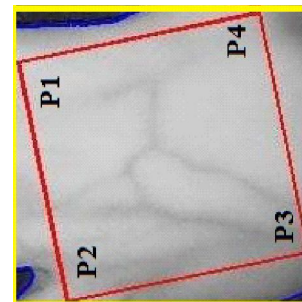
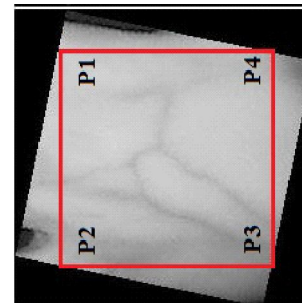


Fig.3 Rotation angle



(a)



(b)



(c)

Fig.4 The process of obtaining a standard orientation ROI from (a) a cropped area, (b) to a rotated ROI at angle θ and (c) the final ROI for later processing.

IV. HAND VEIN PATTERNS IMAGING

In general, several stages are carried out to detect handveins. In the following work five investigated algorithms are:

- A) Histogram Equalization (HE).
- B) Contrast Limited Adaptive Histogram Equalization(CLAHE)
- C) Radon like feature
- D) Jerman Enhancement filter

A) Histogram Equalization (HE)

Histogram equalization is a technique for adjusting image intensities to enhance contrast [6].The transformation function T(r) also called auxiliary function used to perform histogram equalization.

Such transformation function must satisfy two criteria [7]:

1. T (r) must be a monotonically increasing function in the Interval. $0 \leq r \leq L - 1$.
2. $0 \leq T (r) \leq L - 1$ for $0 \leq r \leq L - 1$.

The most usual transformation function is the cumulative distribution function (cdf) of the original probability mass function given by

$$s_k = T(r_k) = \sum_{j=0}^k \frac{n_j}{n} = \sum_{j=0}^k p(r_j)$$

where s_k is the new (mapped) gray level for all pixels whose original gray level used to be r_k . The inverse of this function is given by.

$$r_k = T^{-1}(s_k) \text{ for } k=0,1,\dots,L-1$$



Fig. 5 Contrast enhancement results from hand vein image using HE.

B) CLAHE

As already stated, CLAHE method is an improvement over standard HE. CLAHE generally divides the image into a number of non-overlapping contextual regions unlike HE operates on the whole image. [8]. According to the

size of appropriate regions, histogram is calculated and created independently.

$$H_{ij}(x, s) = s^2 I(x) * \frac{\partial^2}{\partial x_i \partial x_j} G(x, s) \text{ for } i, j = 1, \dots, D,$$

Then, a clip limit value for clipping histograms is determined as a threshold. Next, the histogram is clipped according to the predefined clipping limit. The accessed clipped pixels are then distributed back to the clipped histogram[9]. Finally, the gray level mappings were combined using bilinear interpolation in order to assemble the final enhanced image.



Fig. 6 Contrast enhancement results from hand vein image using CLAHE

C) Radon like features

Radon-Like features, which permit for collection of spatially scattered image measurements into dense feature descriptors.

Following is the transformation function of the input image I(x,y) used to extract radon like feature for hand vein enhancement [11]:

$$R(x, y) = \max_{\sigma, \phi} \Delta G(\sigma, \phi) * I(x, y),$$

To enhance scale and orientation of boundary for Gaussian-Second-Derivative (GSD), σ and Φ are used [14].The knots for Radon-Like features are defined using an edge map of R(x,y) and the extraction function, T_2 , is given as

$$T_2(I, t(t)) = \frac{\int_{t_i}^{t_{i+1}} R(t(t)) \partial t}{\| t(t_{i+1}) - t(t_i) \|}, t \in [t_i, t_{i+1}]$$

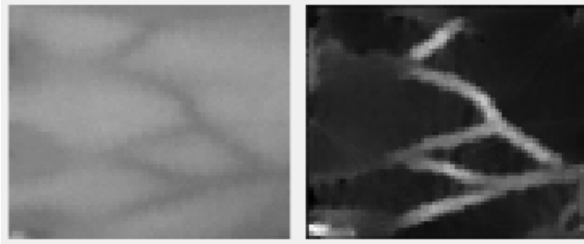


Fig. 7 Contrast enhancement results from hand vein image using Radon like features

D) Jerman Enhancement Filter

This filter is based on multiscale Hessian eigenvalues, which produces a similar response in all the vein pattern and enhances the border between the vein pattern and the background[10].

Enhancement filters are scalar functions $V : R \rightarrow R$, which selectively amplify a specific local intensity profile or structure in an image. Some of the image enhancement filters describes local structure by evaluating hessian or second order intensity derivative at each and every point in the image[15]. To enhance the local structures of various sizes, the analysis is typically performed on a Gaussian scale space of the image.

The $I(x)$ represent the intensity of a D-dimensional image at coordinate $x = [x_1, \dots, x_D]^T$, then the Hessian of $I(x)$ at scale s is represented by a $D \times D$ matrix defined as:

$$H_{ij}(x, s) = s^2 I(x) * \frac{\partial^2}{\partial x_i \partial x_j} G(x, s) \text{ for } i, j = 1, \dots, D,$$

where $G(x, s) = (2\pi s^2)^{-D/2} \exp(-x^T x / 2s^2)$ is a D-variate Gaussian and * denotes convolution.

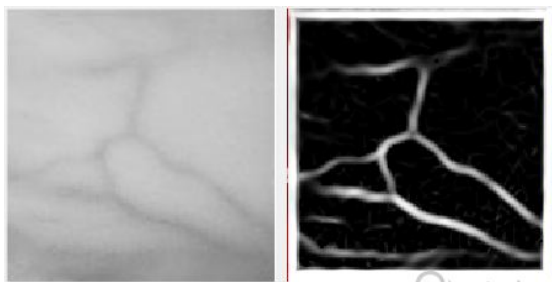


Fig. 2 Contrast enhancement results from hand vein image using Jerman Enhancement filter

V. ENHANCEMENT PERFORMANCE MEASURE AND EXPERIMENTAL RESULTS

There is no universal measure, which specifies both the objective and subjective validity of the enhancement for all

types of images. Contrast, brightness and sharpness are the three basic parameters that control the quality of an image. An image can be described by means of first order statistics of gray values of the pixels inside a neighborhood. Examples of such features extracted from the image histogram are mean, standard deviation (SD) and entropy. The second order features are based on gray level co-occurrence matrix (GLCM) and it is one of the most popular methods for pixel variation statistics [14]. Some of the second order statistical features are entropy, contrast, homogeneity, energy and correlation of the gray level pixels, defined as

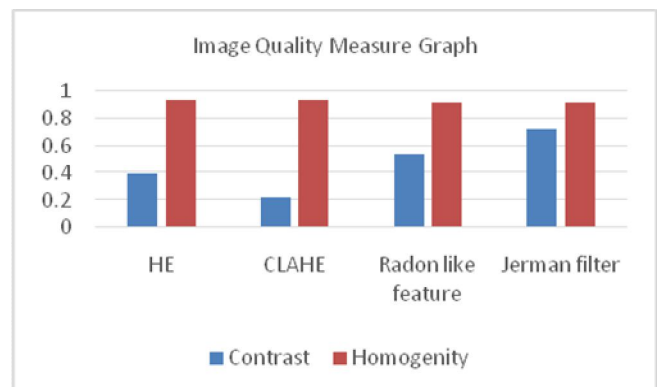
$$contrast = -\sum_i \sum_j (i - j)^2 P(i, j)$$

$$Homogeneity = \sum_i \sum_j \frac{P(i, j)}{1 + |i - j|}$$

where i and j are two different gray levels of the image, P is the number of the co-appearance of gray levels i and j . The similarity of gray-scale levels across the image measures is homogeneity and contrast returns a measure of the intensity difference between a pixel and its neighbor pixel over the whole image. Thus, larger the changes in the grayscale, the higher the contrast and lower the homogeneity.

Table.1 image quality measures for the enhancement technique

	HE	CLAHE	Radon like feature	Jerman filter
Contrast	0.3961	0.2231	0.54	0.7280
Homogeneity	0.9314	0.9312	0.9212	0.9215



VI. CONCLUSION

In this paper, four methods for hand vein image enhancement have been presented. Some of the enhancement systems like Histogram Equalization (HE), Contrast Limited Adaptive Histogram Equalization (CLAHE), Radon-like features (RLF), Jerman enhancement filter, have been implemented and compared. The performance of all these methods has been analyzed and a number of practical experiments of images have been presented. From the experimental results, it is found that all the techniques yield different aspects for different parameters. The efficiency of the proposed method is promising even if the test database used in the experiments is quite small.

REFERENCES

- [1] Han, C.C., Cheng, H.L., Lin, C.L., Fan, K.C., "Personal authentication using palm-print Feature", Elsevier Pattern Recognition vol.36, pp. 371-381, 2003.
- [2] Li, W.X., Zhang, D., Xu, Z.Q., "Image alignment based on invariant features for palmprint Identification", Signal Processing: Image Communication vol.18(5), pp. 373-379, 2003
- [3] Kumar, Wong, D.C.M., Shen, H.C., "Personal verification using palmprint and hand geometry biometric", In: 4th International Conference on Audio and Video-Based Biometric individual Authentication, Guildford, U.K., pp. 668-678, 2005.
- [4] Han, X., Research on algorithm for human dorsal hand vein recognition. Ph.D. Thesis. Jilin University, 2007.
- [5] Y. Zhang, X. Wu, S. Lu, H. Wang, P. Phillips, S. Wang, "Smart detection on abnormal breasts in digital mammography based on contrast-limited adaptive histogram equalization and chaotic adaptive real-coded biogeography-based optimization", SIMULATION, vol. 92, pp. 873-885, 2016.
- [6] Seungjoon Yang, Jae Hwan Oh, and Yungjun Park, "Contrast enhancement using histogram equalization with bin underflow and binoverflow", In: International Conference on Image Processing (ICIP), 2003.
- [7] R. C. Gonzalez and R. E. Woods. "Digital Image Processing", 3rd edition, Prentice Hall, Upper Saddle River, NJ, 2008.
- [8] J. Zhao, X. Xiong, L. Zhang, T. Fu and Y. Zhao, "Study on enhanced algorithm of hand vein image based on CLAHE and Top-hat transform", In: Chinese journal of Laser and Infrared, pp. 220-222, 2009.
- [9] Etta D, Pisano, S. Zong, R. E Jhonston "Contrast limited adaptive histogram equalization image processing to improve the detection of simulated speculation in Dense Monograms", In: Journal of Digital Imaging, vol. 11, No. 4, pp 193-200, 1998.
- [10] A. F. Frangi, W. J. Niessen, K. L. Vincken, and M. A. Viergever. "Multiscale vessel enhancement filtering". In : W. M. Wells, A. Colchester, and S. Delp, editors, MICCAI'98 Medical Image Computing and Computer-Assisted Intervention, Lecture Notes in Computer Science, Springer Verlag, pp. 130–137, 1998.
- [11] Ritwik Kumar, Amelio Vazquez-Reina and Hanspeter Pfister, "Radon-Like Features and their Application to Connectomics", In: IEEE Computer Society Conference on Computer Vision and Pattern Recognition Workshops (CVPRW), 2010.
- [12] A. Djerouni, H. Hamada and N. Berrached "MR imaging contrast enhancement and segmentation using fuzzy clustering" In: IJCSI International Journal of Computer Science Issues, Vol. 8, Issue 4, No 1, pp. 286-290, 2011.
- [13] C. Nageswara Rao, S. Sreehari Sastry, K. Mallika, Ha Sie Tiong and K. B. Mahalakshmi. "Co-Occurrence Matrix and Its Statistical Features as an Approach for Identification of Phase Transitions of Mesogens" In: IJRSET International Journal of Innovative Research in Science Engineering and Technology Vol. 2, Issue 9, 2013.
- [14] S. R. Deans. The Radon Transform and Some of Its Applications John Wiley and Sons, 1983.
- [15] Tim Jerman, Franjo Pernus, Bostjan Likar, and Ziga Spiclin, "Beyond Frangi: an improved multiscale vesselness filter, Proc. of SPIE Vol. 9413, pp. 94132A-1 94132A-13, 2015.